Chapter 2
3D Tracking of Respiratory Liver Movement by a Robot Assisted Medical Ultrasound

Ryu Nakadate, Ammar Safwan, Hiroyuki Ishii, Akiko Saito, Atsuo Takanishi, and Makoto Hashizume

Abstract It is often required to hold an ultrasound probe for long time so that the moving target is maintained within the B-mode image, especially for minimally invasive interventions. Using a conventional 2D probe, the tracking out-of-plane motion is a challenging technique because in this case the target is missing from the image plane. In this paper, we propose a 3D tracking method for a probe holding robot based on the 2D B-mode image feedback. In order to track the out-of-plane motion, a template matching between the current image and the previously recorded 3D data is performed. In-plane motion is detected by a template matching in the plane. Essentially the tracking by visual information on the real soft tissue is difficult because of its deformation. However, our method is robust for a certain amount of the deformation. We have applied this method for an in-vivo experiment of human liver respiratory motion compensation and results show its effectiveness.

Keywords Ultrasound • Robotics • Visual servoing

2.1 Introduction

During the therapy or diagnosis by using medical ultrasound imaging system, keeping the same cross section by holding a probe for long time is sometimes required. For example, during the micro-bubble contrast enhanced ultrasound, the probe has to be held at the target point (i.e. liver) for more than 20 min [1]. During the flow-mediated dilation diagnosis, which is used for the diagnosis of the arteriosclerosis, fine images of the longitudinal section of the brachial artery have to be

R. Nakadate (✉) • M. Hashizume
Center for Advanced Medical Innovation, Kyushu University, Fukuoka, Japan
e-mail: nakadate@camiku.kyushu-u.ac.jp

A. Safwan • H. Ishii • A. Takanishi
Faculty of Science and Engineering and Humanoid Robotics Institute, Waseda University, Tokyo, Japan

A. Saito
Institute of Gastroenterology, Tokyo Women's Medical University, Tokyo, Japan

M.G. Fujie (ed.), *Computer Aided Surgery*, DOI 10.1007/978-4-431-55810-1_2

kept for up to 10 min [2]. The needle insertion therapy under the ultrasound guide also requires the same skill. Ultrasound guide is also used for the high intensity focused ultrasound therapy (HIFU) [3]. In such tasks, if the operator holds the probe, it will interrupt the other task of the operator. If a therapy requires a very accurate positioning of the probe, the tremor of the operator's hand will be a problem. The mechanical probe holder is sometimes used, but in this case the patient motion will be the problem.

There are some past researches for the image guided target tracking by using a robot assisted ultrasound system using B-mode images. Normal, prevailing probes obtain two dimensional images of a cross section of organ. Detection of the movements of the target in-plane (translational movement in x, y axis and rotational movement in z axis in Fig. 2.1) is relatively easy. But out-of-plane motions (translational z axis and rotational x, y axis) are difficult to be detected because in those case the target disappears from the image. In the literature, in-plane target tracking by using ultrasound B-mode image is applied for the tracking of the cross section of carotid artery [4], bladder [5], etc. Many methods in the image processing techniques, such as template matching and contour detection can be used for the target detection. However, those methods can not be used for the out-of-plane motion because the target disappears from the image.

A three dimensional target tracking system by using orthogonally aligned two probes was proposed in [6]. However, most of the commercialized medical ultrasound systems do not allow using two probes at once. The matrix array probe which can obtain volume data is available but for only a limited type of the probe. A method for measuring the distance of two parallel images by using image

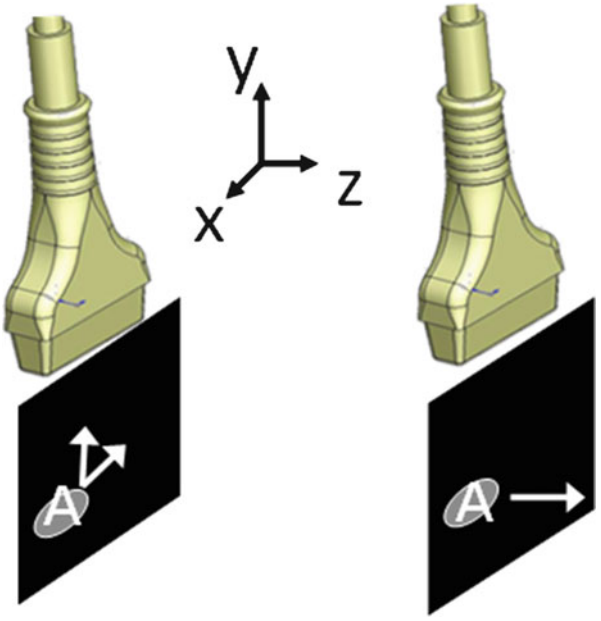

Fig. 2.1 In-plane motion (*left*) and out-of-plane motion (*right*)

correlation was proposed in [7]. But this method can not detect the direction of the movement. Similarly, [8] used three parallel frames containing two fiducial frames and one target frame. By comparing the distance from each fiducial frame to the target, the direction can be detected. But this study demonstrated only phantom test, not in the real tissue. The application for the real tissue is challenging because those methods are based on the rigid, non-deformable motion of the target. The authors have proposed the robust algorithm for out-of-plane motion tracking by using B-mode image of a single probe [9]. This method utilizes the volume data around the target obtained before tracking. The image correlation is used to estimate the target position. Our method is relatively robust for the real application because it utilizes large prior information such as volume data.

In this paper, in order to verify the possibility of the application of our method for the surgical tasks, this method is applied for the tracking of the human liver respiratory motion. The liver is chosen as the target because it is suitable for the preliminary experiment. It is solid organ, large enough for the region of interest (ROI) setting, and has large movement by respiration.

2.2 Method

This section describes the tracking algorithm which includes one axis of out-of-plane motion and two axes of in-plane motions. The first step is scanning the small section around the target by the probe held by the robot, and recording the consecutive B-mode images with position data. By this step, 3D data which center is the target is obtained. This step is done once just before target tracking. The second step is tracking. During tracking, the B-mode image obtained by the probe is matched in the 3D data by using image correlation. The position error is the vector from the center of the 3D data to the matched position. The position error is compensated by moving the probe by the robot. The details of the algorithm is as follows; (as shown in Fig. 2.2)

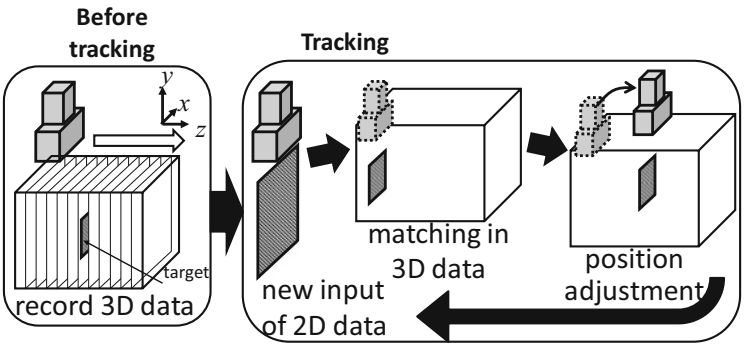

Fig. 2.2 Proposed method of out-of-plane motion detection

1. Manually operate the robot which holds the probe so that the target is observed in the B-mode image. This position is called starting position.
2. The robot moves -*LN*/2 in z axis from the starting position, then moves *LN* in z axis recording the consecutive N parallel frames at a regular interval L, finally go back to the starting position.
3. (start tracking) A rectangular ROI (size $n \times m$ pixels) is set as a template in the current B-mode image. This ROI had better include the target object.
4. Template matching is performed between the above template and all N frames. The sum of squared difference (*SSD*) was used as the image correlation. *SSD* is given by Eq. (2.1);

$$SSD = \sum_{j=1}^{m} \sum_{i=1}^{n} \{I_k(x+i, y+j) - I_c(i,j)\}^2 \tag{2.1}$$

, where I_k is the grayscale (0–255) in the k^{th} frame, I_c is the grayscale of the template in the current frame, and x, y are the coordinate in the frames.
5. As a result, matched position x, y in all frames where *SSD* is smallest and its *SSD* value are acquired. They are defined as $x(k)$, $y(k)$, $SSD(k)$ respectively.
6. The frame number k with the minimum $SSD(k)$ among all frames is defined as k_{match}. The relative position of the probe (X, Y, Z) from the target is given by Eq. (2.2) (2.3) and (2.4).

$$X = sx(k_{match}) \tag{2.2}$$

$$Y = sy(k_{match}) \tag{2.3}$$

$$Z = \left(k_{match} - \frac{N}{2}\right)L \tag{2.4}$$

, where s is the pixel size.
7. The velocity command V_x, V_y, V_z are given to the robot as Eq. (2.5)

$$Vx = \alpha X, Vy = \beta Y, Vz = \gamma Z \tag{2.5}$$

, where α, β, γ are the feedback gain.

2.3 Preliminary Experiments

2.3.1 Distance of the Liver Movement

As a preliminary study, the liver movement including distance and direction are measured by observation of the ultrasound images. We assume the liver moves along the body trunk by the motion of the diaphragm. Therefore we obtained the

ultrasound B-mode images which are parallel to the body trunk, observed the liver movement in those images.

As shown in Fig. 2.3a, ultrasound images are recorded at three positions, (A) just under the epigastrium, (B) 50 mm from A, (C) 80 mm from A. The probe is held by the robot with no movement. The subject is a healthy male, age 40. After starting recording, one respiratory cycle is extracted. At the first frame (beginning of the respiration), several templates are set on the image. In the following frames, the trajectories of those templates are obtained by performing template match. The result is shown in Table 2.1. Samples of the trajectory are shown in Fig. 2.3b. In the cross section A, five points in the liver are measured. In the cross section B and C, three and one points are measured respectively. In all nine points, maximum travelling distance was 18 mm in x axis. Although it is a small, the movement in y axis was also observed.

2.3.2 *Tracking Axis*

For the tracking of the human liver, the best probe position is where the large portion of the cross section is occupied by the liver image. Such position is the right subcostal area (just under the costal bone), the probe orientation is parallel to the edge of the costal bones. In this position, the scanning by the probe had better be the pivot scanning than the parallel scanning (Fig. 2.4). Therefore, the tracking algorithm for the translational x, y, z axis described in Sect. 2.2 is replaced by the one for the translational x, y and rotational x (θ). According to this, the regular interval L, the position Z, velocity V_z are replaced by the angular variables. The initial scanning for recording 3D data (step 2 of the Sect. 2.2) is also to be done with the pivot movement. All other algorithm remains the same. The pivot angle for

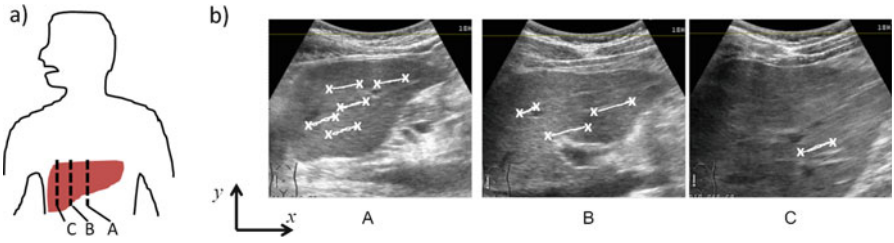

Fig. 2.3 (**a**) Positions for the liver movement measurement test, (**b**) Example of the movement of the liver

Table 2.1 Respiratory movement of the liver

	Average	SD	Max.
Distance x[mm]	15.0	1.8	18.2
Distance y[mm]	4.4	1.4	6.0

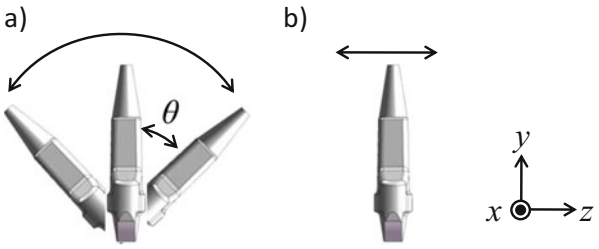

Fig. 2.4 (**a**) Pivot scanning, (**b**) and parallel scanning

initial scanning *LN* is set as ±10°. In this case, the scanning distance at the depth 50 mm (the center of the image) is 17.5 mm.

2.4 Experiment and Result

The proposed method is applied for a real human. The subject is a healthy male, age 40. A industrial robot with six degrees of freedom, MELFA RV-1A (Mitsubishi electric corporation, Japan) is used. The robot holds the 3.75 MHz convex probe which is connected to the ultrasound imaging device Pro Sound II SSD-6500SV (Hitachi-Aloka medical, Japan). The NTSC signal output from the imaging device is led into the PC (Core i7, 2.9 GHz) through video capture unit PCA-DAV2 (Princeton, Japan). The image processing software is based on the OpenCV. The number of recorded frames before tracking *N* is set as 20. The frame rate of both the ultrasound imaging device and image processing in PC are 30 frames per second. The target velocity at the tip of the probe given in Eq. (2.5) is integrated into position command, and then sent to the position controlled robot. The subject is laid on the bed in supine position. During the step 1 and 2 in the Sect. 2.2, the subject holds the breath. The experimental setup is shown in Fig. 2.5. The longitudinal section of the portal vein is chosen as the target object. The diameter of this object was 8.9 mm. The definite validation requires the grand truth of the absolute position of the object. However, it is not available in non-invasive way. Therefore verification of the tracking is done by whether the shape of the object is always kept in the image during the tracking.

Figure 2.6 shows the consecutive B-mode image during one cycle of the respiration. The above figures are images during tracking, bottom figures are images without tracking. Left end is the beginning of the inspiration. The third image in the top row and the forth image in the bottom row are corresponding to the begging of the expiration. Right end is the end of the expiration. In the case of without tracking, at the end of the inspiration period, the shape of the portal vein is disappeared, while the tracking case keeps its shape in all images. The movement of

Fig. 2.5 Experimental setup of the liver tracking

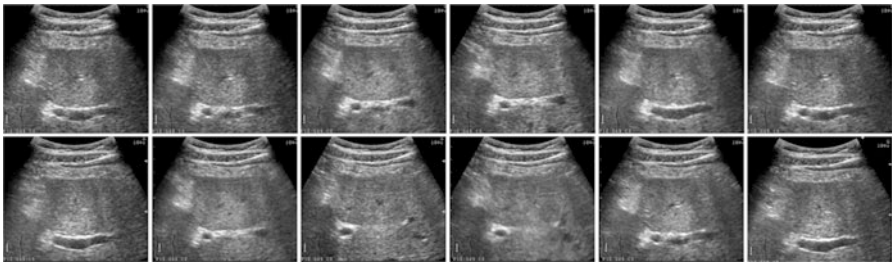

Fig. 2.6 The B-mode image of one respiratory cycle with tracking (*top*), without tracking (*bottom*). From *left*, t = 0, 0.7, 1.4, 2.1, 2.8, 3.5[s] from the begging of the inspiration. Third image in the top row and the forth image in the bottom row are corresponding to the begging of the expiration

the tip of the probe is shown in Fig. 2.7. The out-of-plane motion is calculated as 14 mm from the magnitude of the θ, 10° and depth of the target 80 mm. This is nearly equals to maximum liver motion 15 mm which is measured in the Sect. 2.3. Horizontal x and vertical y movements of the probe were 3 mm, 10 mm respectively. Figure 2.8 shows the tracking error which is determined by only the image processing.

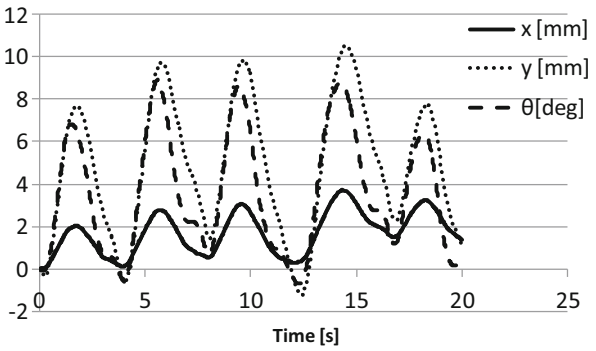

Fig. 2.7 Trajectory of the probe during the tracking

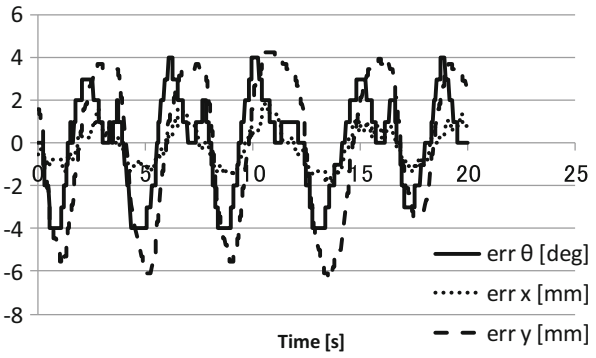

Fig. 2.8 Tracking error (detected relative position of the probe against the image)

In the experiment, the maximum time of the consecutive tracking until the target is missing was measured for three times. The result was 4 min 34 s ±20 s (average ± SD).

2.5 Discussion

The horizontal and vertical movement in Fig. 2.7 is slightly larger than the liver movement measured in Sect. 2.3. One reason is that the experiment in Sect. 2.3 is not considering the body face motion by respiration. According to the Fig. 2.8, the maximum tracking error of θ is 4°. This is equal to about 5.6 mm at the depth of 80 mm. It is the reason why the target object partially drops out from the image. One reason of the tracking error might be the delay in both the control cycle of the robot and the latency for the video capture. The control cycle of the robot is limited by the firmware of the industrial robot. It can be dramatically improved by building own robot. The latency is depends on the capture device. The best way is directly access the RF signal in the ultrasound imaging device, if possible. In our case, the commercialized ultrasound device did not allow such direct access to the inside.

The maximum duration about 4 min was still not enough for the real application. We assume that its limit was caused by the deformation of the tissue and therefore the template match did not reach at the optimal solution. In order to aim at the further robustness, for example, refresh the 3D data during the tracking is one of the choices. At the moment we use only the brightness information. Any feature which is robust to the deformation is desired. Those are our future work.

Acknowledgments This work was supported by JSPS KAKENHI Grant Number 25350568.

References

1. Hatanaka, K., Kudo, M., Minami, Y., Ueda, T., Tatsumi, C., Kitai, S., Takahashi, S., Inoue, T., Hagiwara, S., Chung, H., Ueshima, K., Maekawa, K.: Differential diagnosis of hepatic tumors: value of contrast-enhanced harmonic sonography using the newly developed contrast agent, Sonazoid. Intervirology **51**(Suppl. 1), 61–69 (2008)
2. Playford, D.A., Watts, G.F.: Non-invasive measurement of endothelial function. Clin. Exp. Pharmacol. Physiol. **25**, 640–643 (1998)
3. Orsi, F., Arnone, P., Chen, W., Zhang, L.: High intensity focused ultrasound ablation: a new therapeutic option for solid tumors. J. Cancer Res. Ther. **6**(4), 414–420 (2010)
4. Abolmaesumi, P., Salcudean, S.E., Zhu, W.H., Sirouspour, M.R., DiMaio, S.P.: Image-guided control of a robot for medical ultrasound. IEEE Trans. Robot. Autom. **18**(1), 11–23 (2002)
5. Aoki, Y., Kaneko, K., Oyamada, M., Takachi, Y., Masuda, K.: Probe scanning support system by a parallel mechanism for robotic echography. IEEJ Trans. Electron. Inform. Syst. **130**(3), 433–441 (2010)
6. Koizumi, N., Lee, D., Ota, K., Yoshizawa, S., Yoshinaka, K., Matsumoto, Y., Mitsuishi, M.: A framework of the non-invasive ultrasound theragnostic system. Lect. Notes Comput. Sci. **5128**, 231–240 (2008)
7. Prager, R.W., Gee, A.H., Treece, G.M., Cash, C.J.C., Berman, L.H.: Sensorless freehand 3-D ultrasound using regression of the echo intensity. Ultrasound Med. Biol. **3**, 437–446 (2003)
8. Krupa, A., Fichtinger, G., Hager, G.D.: Real-time motion stabilization with B-mode ultrasound using image speckle information and visual servoing. Int. J. Robot. Res. **2009**(10), 1334–1354 (2009)
9. Nakadate, R., Solis, J., Takanishi, A., Minagawa, E., Sugawara, M., Niki, K.: Out-of-plane visual servoing method for tracking the carotid artery with a robot-assisted ultrasound diagnostic system. In Proc. of 2011 IEEE Int. Conf. on Robotics and Automation (ICRA), pp. 5267–5272 (2011)

http://www.springer.com/978-4-431-55808-8

Computer Aided Surgery
Fujie, M.G. (Ed.)
2016, XII, 148 p. 100 illus., 27 illus. in color., Hardcover
ISBN: 978-4-431-55808-8